
GAZEVLM: A VISION-LANGUAGE MODEL FOR MULTI-TASK GAZE UNDERSTANDING

A PREPRINT

Athul M. Mathew*, Haithem Hermassi, Thariq Khalid, and Arshad Ali Khan

Applied Research, Elm Company, Saudi Arabia

March 17, 2026

ABSTRACT

Gaze understanding unifies the detection of people, their gaze targets, and objects of interest into a single framework, offering critical insights into visual attention and intent estimation. Prior methods have modelled gaze cues in visual scenes, but a unified system is still needed for gaze understanding using both visual and language prompts. This paper introduces GazeVLM, a novel Vision-Language Model (VLM) for multi-task gaze understanding in images, addressing person detection, gaze target detection, and gaze object identification. Unlike other transformer-based methods, GazeVLM represents the first application of a VLM to these combined tasks, allowing for selective execution of each task. Our ablation study on visual input combinations reveals that a fusion of RGB images with HHA-encoded depth maps, guided by text prompts, yields superior performance. We also introduce an object-level gaze detection metric for gaze object identification (AP_{ob}). Through experiments, GazeVLM demonstrates significant improvements, achieving state-of-the-art evaluation scores on GazeFollow and VideoAttentionTarget datasets.

1 Introduction

Humans possess a remarkable ability to track eye gaze, enabling them to interpret focus and predict actions [1]. Gaze offers critical insights into attention, cognition, and intent, serving as a powerful nonverbal cue that reveals visual focus and communicates interests [2]. This has made gaze behaviour a key area of study across disciplines to better understand human attention and behaviour. Understanding human gaze is critical for developing intelligent systems capable of seamless human interaction. Teaching machines to accurately estimate gaze is a significant challenge [2].

Gaze understanding, the task of determining where and what a person looks at in everyday images, sits at the center of human-centric computer vision and directly impacts human-computer interaction, assistive perception, social signal analysis, and embodied AI [3, 4]. In third-person imagery, progress hinges on solving three questions together: who is the subject, where in the scene the gaze lands, and what object or region receives attention. These questions are entangled because gaze depends on subtle ocular and facial cues while also being shaped by scene geometry and semantics. Treating them jointly is natural; doing so robustly is difficult. Reliability in the wild remains difficult. Occlusions from hair or glasses, strong head-pose variation, and non-uniform lighting degrade facial evidence, while out-of-frame gaze targets break image-local heuristics [5]. Error cascades are common: a near-miss in person localization shifts the crop, the head pose becomes slightly biased, and the downstream gaze heatmap drifts toward a salient but irrelevant object. The result looks plausible, but is wrong. These brittleness patterns motivate models that reason across appearance and geometry while preserving the interdependence among detection, target localization, and object identification. In this paper, we aim to bridge these three fundamental and intertwined tasks for gaze understanding using a single unified model - GazeVLM.

Recent works, such as Gaze-LLE [6], have explored the use of foundation models for gaze target detection. However, such methods do not incorporate person detection or gaze objects. Similar to prior methods, this research [6] employs

*Corresponding author: amathew@elm.sa

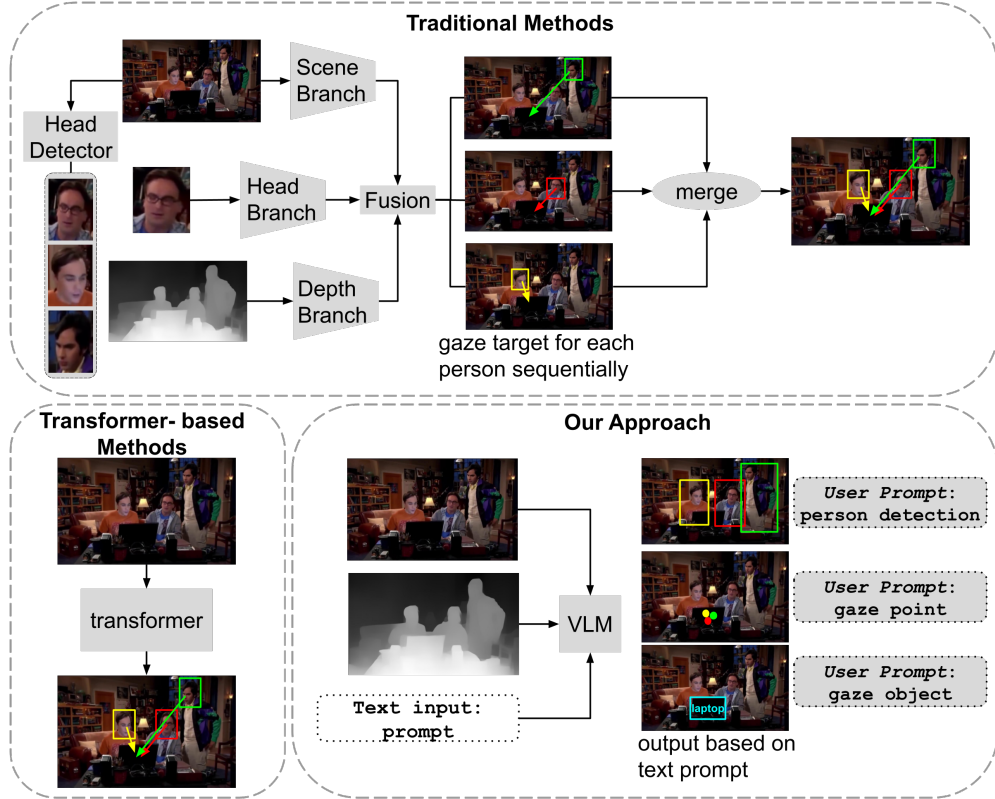


Figure 1: A comparison of previous methods versus our approach.

scene parsing, but with the key distinction that it makes use of DinoV2 transformer instead of CNN-based backbones used by the previous methods. Furthermore, Gaze-LLE [6] requires an additional input—the head location—predicted by a separate model, which adds dependency and complexity to the pipeline.

Recently, Vision Language Models (VLM) are playing a big role in the convergence of Computer Vision and Large Language Models. They serve as a way to query and understand what is happening in images and videos using natural language as the foundation. VLMs are advanced AI models that blend computer vision and natural language processing, learning joint representations of images and text. VLMs excel at learning rich representations of visual and linguistic information, enabling them to perform a wide range of tasks, including image captioning, visual question answering, and object detection. There have been many generic VLMs as well as domain-specific VLMs in recent research spaces.

VLMs have emerged as powerful tools for multimodal understanding, offering a promising new direction to address tasks. Recent efforts have explored integrating human gaze as an additional modality to align model attention with user intention [7]. For instance, a recent study demonstrated that prompting a VLM to describe scenes automatically captures relevant contextual information—such as objects, people, body poses, and interactions—thereby enhancing gaze prediction and improving generalization to unseen scenarios [8]. This highlights the potential of VLMs to enhance contextual awareness in gaze modelling. For example, understanding that “person A is pointing at an object” or “person B is speaking” provides valuable context for predicting where person C might look [8].

1.1 GazeVLM

Figure 1 presents a high-level comparison between the existing methods and our approach. Building on the success of VLMs, we introduce GazeVLM, a novel approach to gaze understanding using VLM. Fine-tuned from Qwen2.5-VL [9], GazeVLM generalizes across person detection, gaze target detection, and gaze object identification. Its architecture includes a vision tower to extract high-dimensional embeddings from RGB images and HHA-encoded (Horizontal disparity, Height and Angle) depth maps, followed by a cross-attention fusion module that integrates visual and geometric cues. The fused representation is processed by a text decoder to generate task-specific predictions, enabling robust gaze analytics. Unlike prior methods relying on visual features alone, GazeVLM’s multimodal design

enhances accuracy and robustness, particularly in challenging scenarios like occlusions, out-of-frame gaze targets, and ambiguous contexts.

1.2 Our contribution

This paper introduces a novel approach for gaze understanding. Our key contributions are as follows:

1. **The first VLM-Based Framework for Unified Gaze Understanding:** To our knowledge, this is the first work to incorporate a vision–language model for unified gaze understanding. Unlike prior single-task methods that rely on traditional single-branch and multi-branch fusion methods, GazeVLM supports a multi-task learning setup encompassing person detection, gaze target detection, and gaze object identification.
2. **Efficient Depth Modality Integration via HHA Encoding:** We represent depth maps as HHA encodings to ensure better compatibility with the pretrained vision tower. Our contribution lies in designing a novel approach that enables both RGB and depth modalities to be processed through the same frozen vision encoder.
3. **GazeVLM Dataset:** We introduce a novel dataset that is prepared and curated from datasets like GazeFollow [1] and VideoAttentionTarget [10] for VLM adaptation. GazeVLM dataset is made available to the research community to facilitate further progress in this area.

In the following sections, we outline the structure of this paper: Section 2 reviews prior work in gaze understanding and multi-modal VLM applications. Section 3 discusses dataset preparation for GazeVLM. Section 4 elaborates on our multimodal approach and training methodology. Section 5 evaluates GazeVLM on *gaze target detection* and *gaze object identification* tasks. Finally, Section 6 provides concluding remarks and Section 7 identifies future directions.

2 Related Work

2.1 Single and multi-branch methods

Gaze target detection has been predominantly addressed through multi-branch fusion models [2, 11–16], where an encoder is followed by parallel branches designed to extract specific gaze-related cues. In contrast, single-branch methods [6, 17, 18] utilize a feature extractor or visual encoder followed by a gaze regression module, prioritizing simplicity but potentially missing nuanced cues. Recent transformer-based architectures, such as TransGOP [11], enhance gaze-object relationship modelling by combining an object detector, a gaze autoencoder, and an object-to-gaze cross-attention mechanism. While this approach demonstrates improved heatmap regression, its performance remains heavily reliant on the accuracy of the underlying object detector. Similarly, GaTector [12] faced challenges in accurately localizing gaze boxes due to limitations in its object detection capabilities, highlighting the critical role of robust object detection in gaze estimation tasks. UVAGaze [16] improved performance through multi-view unsupervised gaze estimation but faced challenges with occlusion and deformation. On the other hand, Liang *et al.* [19] addressed data scarcity by combining multiple datasets across multiple branches, achieving improved generalization. Despite its benefits, this approach faced limitations due to inconsistencies in annotations across datasets.

Recently, single-branch gaze estimation methods [6, 17, 20, 21] have received limited attention in research. Jindal *et al.* [17] proposed an attention mechanism that dynamically adapts to spatial variations across sequential frames and incorporates a bias correction model using pre-trained Gaussian processes. However, this method struggles with long-term spatial and temporal dynamics. Similarly, Gaze-LLE [6] employs a single-branch DINOv2 encoder followed by a head-prompting decoder. Although computationally efficient, its performance depends heavily on the encoder’s size and quality, and it fails to capture diverse gaze-related cues such as head pose, eye movement, and contextual scene information, leading to lower accuracy. Another study [21] introduced a transformer-based model to address the limitations of using head images as input. While achieving promising results, their approaches suffer from slow convergence when focusing on sparse, meaningful locations.

2.2 Single and multi-modal methods

Multi-modal methods [22–29] typically follow a two-stage approach. In the first stage, task-specific predictors extract additional cues, such as depth and pose, to compensate for missing human-scene interactions. In the second stage, the extracted visual and multimodal features are combined, and a decoder predicts the gaze target heatmap. For instance, Athul *et al.* [28] proposed a method that fuses 3D depth estimation, saliency mapping, and multimodal features. However, their approach performs frame-wise predictions and does not account for temporal dependencies. Chen *et al.* [29] introduced a gaze-assisted object referring framework that simplifies existing methods by integrating gaze heatmaps with one-stage object detection and language support. Despite its innovation, their approach was computationally

inefficient and struggled to handle diverse imaging modalities. Gupta *et al.* [25] addressed this limitation by extracting depth and pose maps from input images and combining them into modality saliency feature maps. While effective, their method incurs increased latency, impacting real-time performance.

Unlike multi-modal methods, single-modal approaches [12, 20, 30, 31] often suffer from limited feature representations. ViTGaze [32] introduces a single-modality gaze-following framework that leverages vision transformers (ViTs) to model human-scene interactions through self-attention. Unlike traditional two-stage or complex decoder-based approaches, it focuses on powerful encoders with minimal decoder parameters, simplifying the architecture. To address challenges such as head pose variation and illumination, Shi *et al.* [30] proposed the Agent-guided Gaze Estimation Network (AGE-Net). This framework uses a main branch to capture eye features from low-level semantics, while agent regression tasks refine asymmetry using high-level semantics. Haldun *et al.* [20] introduced U-Net Frame-to-Gaze, a method that predicts 3D gaze origin and direction directly from raw RGB camera frames without requiring eye or face cropping. However, it relies on prior knowledge of camera-to-screen geometry and suggests few-shot learning to adapt to new setups with minimal user input. ESCNet [33] explicitly models 3D geometry by reconstructing the entire scene from a single RGB image and incorporates 3D gaze and scene contextual cues for predictions. While effective, this method requires high input resolution for accurate 3D scene reconstruction.

2.3 Vision language-based methods

Vision Language Models (VLMs) have demonstrated impressive zero-shot performance across various vision tasks. However, accurate gaze following requires capturing contextual cues specific to each individual in the scene. Recent work [8] explores the use of VLMs for extracting zero-shot contextual cues to improve gaze following. Among these, BLIP-2 [34] achieves the best performance, leveraging in-context learning and prompt ensembling to enhance robustness. Using full images with an ellipse around the target improves visual prompting, leading to better generalization. However, the set of cues considered is fixed and depends on the chosen model. Gazeformer [23] introduced ZeroGaze, a novel zero-shot gaze prediction task for unseen objects, and a transformer-based model that utilizes natural language encoding instead of object detectors. With five times faster performance, Gazeformer jointly embeds visual semantic features within language model features to predict human scanpaths for visual search. Indeed, VLMs have shown strong performance in many human-centric tasks, such as action recognition, person re-identification, and search [35]. However, only a few works have addressed gaze understanding. For instance, Yang *et al.* [36] tackle gaze object prediction from an image segmentation perspective by leveraging pixel-level supervision provided vision foundation model. Their method relies on box supervision as prompts for SAM to generate masks, restricting its applicability in scenarios without strong location priors.

3 Dataset

GazeVLM addresses key tasks for third-person human-centric gaze systems, including person detection, gaze point regression, and gaze object localization and classification. It is trained and evaluated on two widely used datasets: GazeFollow [1] and VideoAttentionTarget [10].

GazeFollow is a large-scale static image dataset with 122,143 images and 130,339 head-target annotations, including a test set of 4,782 images. Each gaze target is annotated by ten individuals, ensuring robust ground truth. The dataset focuses primarily on in-frame gaze targets. VideoAttentionTarget extends gaze detection to video sequences, containing 1,331 clips 109,574 in-frame gaze targets and 54,967 out-of-frame gaze annotations. Its test set includes 31,978 gaze annotations from 10 different shows. The dataset is notable for its complexity, featuring multiple head-target annotations per frame, making it ideal for modelling multi-person gaze interactions.

Together, these datasets provide a comprehensive foundation for gaze target detection research across static and dynamic scenarios, significantly advancing the field and serving as valuable resources for researchers.

3.1 Data Preparation

In our approach to leverage datasets for vision-language models, we transformed the original annotations into a text format suitable for the GazeVLM architecture. The GazeFollow dataset contains free-style images with multiple people, where the gaze of selected individuals is evaluated as part of the test set. To estimate the gaze of a specific person, we embed the face location of that individual into the text prompt. Additionally, to identify the gazed object, we extend the GazeFollow dataset with object annotations. We employ Detic [38] object detection model pre-trained on the LVIS dataset [39], which provides a rich vocabulary of 1200 object classes. This choice, over a closed-vocabulary detector, allows us to identify a wider and more diverse range of potential gaze targets without being limited to a predefined, fixed set of object categories. This is particularly beneficial in unconstrained real-world images where the

Task : Person Detection
<pre> <lim_start>user < vision_start>rgb.jpg< vision_end>< vision_start>depth.jpg< vision_end>I'm curious about the photo. Can you locate all the people<lim_end> <lim_start>assistant In the image, there is a < ref_start>person< ref_end>< box_start>(x_{p1}, y_{p1}),(x_{p2}, y_{p2})< box_end><lim_end> </pre>
Task : Gaze Target Point
<pre> <lim_start>user < vision_start>rgb.jpg< vision_end>< vision_start>depth.jpg< vision_end>Please find the < ref_start> person < ref_end> < box_start> (x_{p1}, y_{p1}),(x_{p2}, y_{p2})< box_end> gaze<lim_end> <lim_start>assistant In the image, a < ref_start>person< ref_end>< box_start>(x_{p1}, y_{p1}),(x_{p2}, y_{p2})< box_end>is looking at this < ref_start>gaze point < ref_end>< box_start>(x_{g1}, y_{g1}),(x_{g2}, y_{g2})< box_end><lim_end> </pre>
Task : Gaze Object Detection
<pre> <lim_start>user < vision_start>rgb.jpg< vision_end>< vision_start>depth.jpg< vision_end>What is the object at the < ref_start>gaze point < ref_end> < box_start> (x_{g1}, y_{g1}),(x_{g2}, y_{g2})< box_end><lim_end> <lim_start>assistant In the image, for the < ref_start>gaze point< ref_end>< box_start>(x_{g1}, y_{g1}),(x_{g2}, y_{g2})< box_end>the gaze object is < ref_start> {object class}< ref_end>< box_start>(x_{o1}, y_{o1}),(x_{o2}, y_{o2})< box_end> </pre>

Figure 2: **Dataset format example.** Each task statement is marked with special tokens `<im_start>` and `<im_end>`. Image features are separated from text features using special tokens `<vision_start>` and `<vision_end>`, in line with ChatML [37] format.

gazed objects can be varied and novel. The gazed object is determined by computing the Intersection over Union (IoU) between the gaze point and each detected object:

$$\text{IoU} = \frac{\text{area}(B_{\text{gaze}} \cap B_{\text{obj}})}{\text{area}(B_{\text{gaze}} \cup B_{\text{obj}})} \quad (1)$$

where B_{gaze} is a small bounding box centered on the gaze point, and B_{obj} is the bounding box of a detected object. The object with the highest IoU score is considered the gazed object:

$$O_{\text{gazed}} = \arg \max_{o \in O_{\text{det}}} \text{IoU}(B_{\text{gaze}}, B_o) \quad (2)$$

This approach associates gaze points with specific objects, thus enhancing the semantic understanding of gaze.

To improve the representation of bounding boxes and gaze points in VLMs, we propose an enhanced format based on the convention introduced by [40]. Our approach formalizes bounding boxes in the $xyxy$ configuration, normalized to the range $[0, 1000)$, and represents them as strings:

$$B_{xyxy} = \text{‘ ‘}(x_1, y_1), (x_2, y_2)\text{’ ’} \quad (3)$$

For gaze point estimation, we introduce a transformation to create a bounding box around the gaze point:

$$G_{(x,y)} \rightarrow B_{\text{gaze}} = \text{‘ ‘}(x - \lambda, y - \lambda), (x + \lambda, y + \lambda)\text{’ ’} \quad (4)$$

where $G(x, y)$ is a gaze point, and λ is a fixed margin. To enhance the model’s understanding of spatial representations, we introduce special tokens for formatting bounding boxes:

$$B_{\text{token}} = \text{<box_start>}B_{xyxy}\text{<box_end>} \quad (5)$$

This formatting scheme is applied uniformly to both object bounding boxes (B_{xyxy}) and gaze bounding boxes (B_{gaze}). For associating gazing objects with their corresponding classes, we utilize additional tokens:

$$O_{token} = \langle \text{ref_start} \rangle O_{class} \langle \text{ref_end} \rangle B_{token} \quad (6)$$

where O_{class} is the object class label. The complete representation for a gaze estimation scenario is:

$$S_{gaze} = \langle \text{box_start} \rangle B_{gaze} \langle \text{box_end} \rangle + O_{token} \quad (7)$$

Given Qwen2.5-VL’s inherent inability to directly predict spatial coordinates for grounding, we employ the above formulations to comply with its training data format, thereby facilitating the fine-tuning process for gaze understanding tasks. An example for the dataset format is shown in Figure 2. Additionally, in order to complement GazeVLM with depth understanding, we use monocular depth estimation network from [41] to extract the depth maps from the RGB images.

4 The Methodology

Our work focuses on the task of gaze-related understanding in images, which encompasses three key components: person detection, gaze target detection, and gaze object identification. Given an RGB image $I_{RGB} \in \mathbb{R}^{H \times W \times 3}$ and its corresponding depth map $D \in \mathbb{R}^{H \times W}$, our goal is to predict the gaze target location (x, y) within the image and identify the object being gazed at, even when the object lies outside the image. This formulation allows our model to handle a wide range of real-world scenarios.

4.1 Input Representation

The input to our model consists of two modalities: an rgb image and a depth image. The rgb image provides rich visual information about the scene, while the depth map, encodes geometric information about the relative distances of objects in the scene. Drawing inspiration from [42], we feed HHA geocentric images rather than directly inputting raw depth maps into the vision encoder of the VLM. HHA encoding comprises three components: **Horizontal Disparity (H)**, **Height (H)**, and **Angle (A)**, representing inverse depth, vertical pixel position, and surface orientation relative to the camera, respectively. As discussed in Section 5.3, our rationale is that since vision encoders are predominantly pretrained on RGB images, converting the depth map into a three-channel HHA encoding enhances its compatibility with these pretrained encoders. The structural similarities between HHA geocentric images and RGB images allow the vision encoder, originally designed for RGB data, to effectively extract complementary representations from the HHA images. Our solution enables the extraction of depth-related representations using the vision encoder without the necessity of additional pretraining. Below, we outline the steps to compute the HHA encoding from a depth map $D \in \mathbb{R}^{H \times W}$.

4.1.1 Depth Map Rescaling

First, the depth map D is rescaled to the range $[1, 10]$ to avoid extreme values in the inverse depth computation:

$$D_{\text{rescaled}} = \text{normalize}(D, 1, 10) \quad (8)$$

where $\text{normalize}(\cdot)$ linearly maps the input to the specified range.

4.1.2 Horizontal Disparity (H)

The horizontal disparity channel H is computed as the inverse of the rescaled depth map. To ensure numerical stability, zero values in D_{rescaled} are replaced with a small constant $\epsilon = 10^{-6}$. The resulting H is normalized to the range $[0, 255]$:

$$H = \text{normalize}(1/D_{\text{rescaled}}, 0, 255) \quad (9)$$

4.1.3 Height (H)

The height channel H_{height} is computed based on the vertical position of each pixel in the image:

$$H_{\text{height}} = \left(\frac{y}{H} \right) \times 255 \quad (10)$$

where y is the vertical coordinate of the pixel, and H is the height of the image.

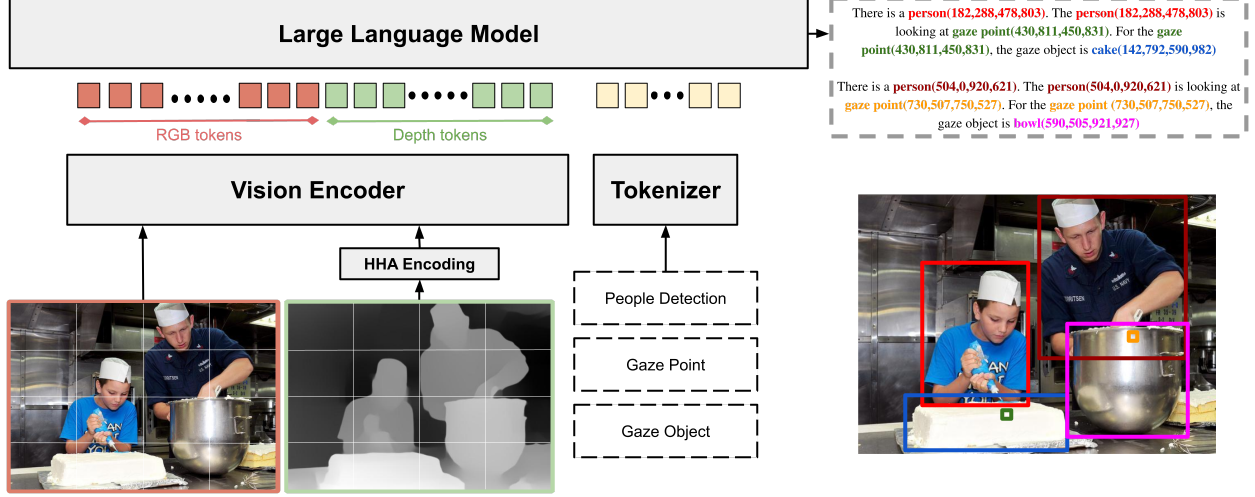


Figure 3: **Overview of GazeVLM.** The model processes an input comprised of an RGB image and a corresponding HHA-encoded depth map. Our model is multi-task and can detect individuals, their gaze points, and the objects they focus on, based on the task provided by the user input prompt.

4.1.4 Surface Normals and Angle (A)

The surface normals \mathbf{n} are computed from the depth map using Sobel operators for gradient computation:

$$\frac{\partial D}{\partial x} = \text{Sobel}(D, \text{axis} = 0), \quad \frac{\partial D}{\partial y} = \text{Sobel}(D, \text{axis} = 1) \quad (11)$$

$$\mathbf{n} = \left[-\frac{\partial D}{\partial x}, -\frac{\partial D}{\partial y}, 1 \right] \quad (12)$$

The normals are then normalized to unit length:

$$\mathbf{n}_{\text{normalized}} = \frac{\mathbf{n}}{\|\mathbf{n}\|_2} \quad (13)$$

The angle channel A is computed as the angle between the surface normal $\mathbf{n}_{\text{normalized}}$ and the camera’s viewing direction $\mathbf{v} = [0, 0, 1]$. The resulting A is normalized to the range $[0, 255]$:

$$A = \text{normalize}(\arccos(\text{clip}(\mathbf{n} \cdot \mathbf{v}, -1, 1)), 0, 255) \quad (14)$$

4.1.5 HHA Encoding

Finally, the simplified HHA encoding is obtained by stacking the three channels:

$$\text{HHA} = \text{stack}(H, H_{\text{height}}, A) \quad (15)$$

4.2 Model Architecture

GazeVLM is built on top of Qwen2.5-VL, which we fine-tune for gaze-related tasks. The model architecture can be seen in Figure 3. It consists of two main components: a vision tower and a text decoder. The vision tower processes the RGB image and the HHA-encoded depth map independently, extracting high-dimensional feature embeddings for each modality. These embeddings alongside text embeddings are then fused using a cross-attention mechanism, which allows to effectively combine visual, geometric and textual information.

4.3 Fusion Strategy

To integrate multimodal inputs, the RGB image (F_{RGB}) and HHA-encoded depth map (F_{HHA}) are independently processed by the vision tower. HHA encoding is adopted to align depth information with the RGB-centric Qwen2.5-VL encoder. These visual embeddings are fused with text embeddings (F_{text}) via cross-attention in the LLM decoder:

$$F_{\text{fused}} = \text{Softmax} \left(\frac{QK^T}{\sqrt{d_k}} \right) V$$

where queries (Q) are projected from F_{text} , and keys (K) and values (V) are derived from the concatenated visual features $F_V = [F_{\text{RGB}}; F_{\text{HHA}}]$. By computing attention between the textual query and the joint visual representation, the model dynamically weights appearance cues from RGB and geometric structures from HHA. This allows the decoder to extract complementary information from either modality based on the specific requirements of the text prompt.

4.4 Training Procedure

We fine-tune the model with GazeFollow and VideoAttentionTarget datasets. Before training, we preprocess the data by converting depth maps to HHA encoding and formatting the datasets to match the input requirements of Qwen2.5-VL as outlined in Section 3.1. We use the 3B variant of Qwen2.5-VL (Qwen2.5-VL-3B-Instruct), AdamW optimizer with a learning rate of $1e-5$ and gradient clipping is applied to ensure stable optimization. Given image I and user input text prompt Q , the model generates answer $A = \{a_1, \dots, a_n\}$. The fine-tuning minimizes the Negative Log-Likelihood of the answer tokens:

$$\mathcal{L} = - \sum_{i=1}^n \log P(a_i | I, Q, a_{<i}) \quad (16)$$

where $P(a_i | I, Q, a_{<i})$ is the probability of token a_i given the input and preceding tokens.

5 Experimentation

5.1 Evaluation Metrics

The evaluation of GazeVLM was conducted across two fundamental gaze-related tasks: **gaze target detection** and **gaze object identification**. The Area Under the Curve (AUC) metric assesses the confidence of the predicted gaze heatmap with respect to the ground-truth gaze data, quantifying how well the predicted heatmap aligns with the actual gaze distribution. The Distance (Dist.) metric calculates the L2 distance (Euclidean distance) between the ground-truth gaze point and the predicted gaze location. To evaluate directional accuracy, the Angle metric is used to measure the angular deviation between the predicted gaze vector and the ground-truth gaze vector. Specifically for the GazeFollow dataset, the minimum Euclidean distance between the predicted gaze point and the ten annotated ground-truth target points for each subject was calculated. In datasets such as VideoAttentionTarget, which include out-of-frame gaze targets, the model’s ability to distinguish between in-frame and out-of-frame gaze was evaluated by calculating the average precision (AP) for out-of-frame gaze probability predictions.

For gaze object detection, the Mean Average Precision (mAP) metric was adopted to assess the model’s performance in object class detection and localization. A prediction is considered correct if the predicted bounding box’s class label matches the ground-truth class label and the Intersection over Union (IoU) between the predicted bounding box and the ground-truth bounding box exceeds a predefined threshold. The IoU, quantifying the spatial overlap between the predicted and ground-truth bounding boxes, was predominantly set to 0.5, reflecting a standard evaluation protocol.

5.2 GazeVLM Evaluation

A comparative analysis against state-of-the-art architectures is shown in Table 1. The method *Random* samples gaze predictions from a standard normal distribution, while *Center* assumes predictions at the image center. *Fixed Bias* reflects dataset biases in face position and gaze fixation points. GazeVLM achieves state-of-the-art scores across all metrics on GazeFollow and VideoAttentionTarget datasets. A significant contribution of this work is the ability of GazeVLM to perform gaze object detection, achieving a competitive mean Average Precision (mAP) metric score of 0.25 on VideoAttentionTarget and 0.23 on GazeFollow datasets.

Figure 4 illustrates GazeVLM’s ability to execute diverse tasks based on specific user prompts. Unlike traditional gaze estimation frameworks that rely on auxiliary networks for head detection, GazeVLM employs a unified, self-contained architecture that achieves performance comparable to, or exceeding, specialized state-of-the-art models. By eliminating the need for external components and auxiliary networks, GazeVLM provides a streamlined, stand-alone solution for multiple gaze-related downstream tasks.

5.3 Ablation Study

To evaluate the impact of HHA depth encoding, we compared three GazeVLM configurations: RGB-only, RGB + depth, and RGB + HHA. As shown in Table 2, the performance of GazeVLM varies across these configurations on

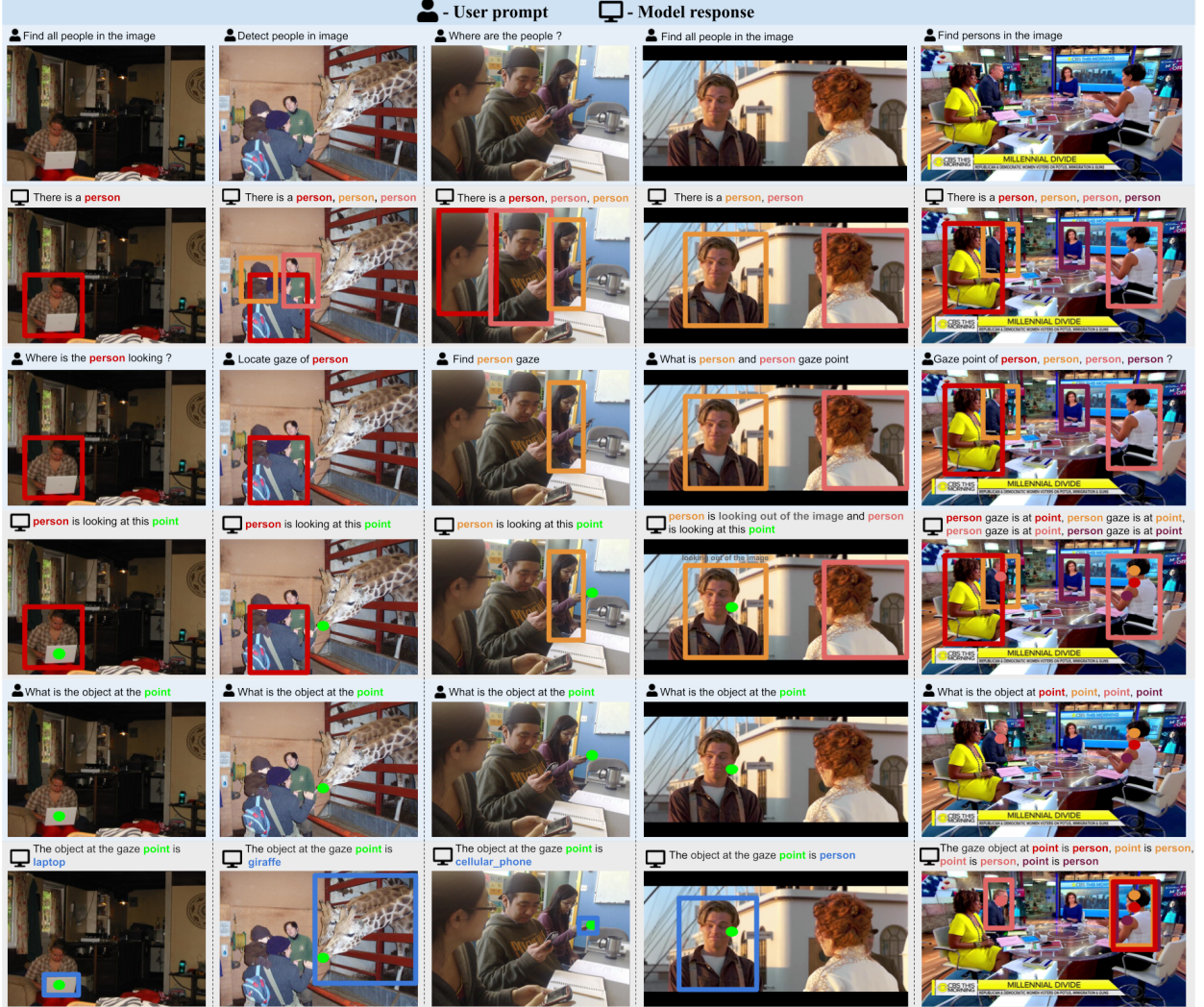


Figure 4: **Qualitative results from GazeFollow and VideoAttentionTarget datasets.** Each column denotes an example image in a series of multi-turn user input prompts and model responses. User input prompt and model response for every image is highlighted row-wise using and respectively. The example in fourth column also demonstrates a scenario for gaze in/out classification. The model responds with a textual tag "looking out of the image" if the person gaze is not within the field of view of the scene image. All model responses are spatially located and color-coded for easier visualization.

the GazeFollow dataset. Interestingly, incorporating raw depth maps with GazeVLM’s frozen vision encoder significantly degraded performance compared to the RGB-only baseline. The inclusion of HHA geocentric images provides essential supplementary information [42] that enhances GazeVLM’s performance. The observation of performance degradation when raw depth maps are used with GazeVLM’s frozen vision encoder is unlike conventional multi-stage networks where depth encoders consistently improved overall accuracy. Pretraining the vision encoder with depth maps could allow the direct use of raw depth maps for better accuracy. However, these results demonstrate that while direct depth integration may require expensive pre-training, HHA provides a computationally efficient alternative that captures essential geometric cues to complement RGB features.

6 Conclusion

GazeVLM represents a significant step towards more accurate and robust gaze understanding. By leveraging the power of VLMs, GazeVLM can effectively integrate vision and text modalities to infer the target of a person’s gaze. This has the potential to revolutionize human-computer interaction, enabling more natural and intuitive communication between

Method	VideoAttentionTarget				GazeFollow				
	<i>AUC</i> \uparrow	<i>Dist.</i> \downarrow	<i>AP</i> \uparrow	<i>AP_{ob}</i> \uparrow	<i>AUC</i> \uparrow	<i>Dist.</i> \downarrow	<i>M.Dist.</i> \downarrow	<i>Angle</i> \downarrow	<i>AP_{ob}</i> \uparrow
Random	0.505	0.458	0.621	-	0.504	0.484	0.391	69.0	-
Center	-	-	-	-	0.633	0.313	0.230	49.0	-
Fixed Bias	0.728	0.326	0.624	-	0.674	0.306	0.219	48.0	-
Recansens [1]	-	-	-	-	0.878	0.190	0.113	24.0	-
Chong [43]	0.830	0.193	0.705	-	0.896	0.187	0.112	-	-
Lian [44]	0.837	0.165	-	-	0.906	0.145	0.081	17.6	-
Danyang [21]	0.893	0.137	0.821	-	0.917	0.133	0.069	-	-
VideoAttn [10]	0.860	0.134	0.853	-	0.921	0.137	0.077	-	-
Fang [45]	0.905	<u>0.108</u>	0.896	-	0.922	0.124	0.067	14.9	-
Jin [21]	0.870	0.127	0.882	-	0.923	0.120	0.064	14.8	-
Tonini [46]	<u>0.940</u>	0.129	-	-	0.927	0.141	-	-	-
Bao [33]	0.885	0.120	0.869	-	0.928	0.122	-	<u>14.6</u>	-
Miao [22]	0.917	0.109	0.908	-	0.934	<u>0.123</u>	0.065	-	-
Tafasca [24]	0.914	0.109	0.834	-	0.939	0.122	<u>0.062</u>	-	-
GazeVLM	0.948	0.102	<u>0.898</u>	0.25	<u>0.936</u>	<u>0.123</u>	0.061	14.2	0.23

Table 1: Evaluation of VideoAttentionTarget and GazeFollow datasets. AP_{ob} is computed for 1200 LVIS vocabulary classes at threshold=0.5. The best and second-best for each metric is represented in **bold** and underline.

Method	<i>AUC</i> \uparrow	<i>Dist.</i> \downarrow	<i>Angle</i> \downarrow
GazeVLM (RGB only)	0.928	0.069	14.5
GazeVLM (RGB+depth)	0.921	0.073	15.1
GazeVLM (RGB+HHA)	0.936	0.061	14.2

Table 2: Comparison of GazeVLM performance under varying configurations of input modalities.

humans and machines. The innovative approach and methodology employed in this research position GazeVLM as a promising solution for diverse applications across AI, robotics, and behavioural research.

7 Limitations and Further Work

Currently, GazeVLM supports only static image-based analysis. It lacks video-based gaze understanding, which limits its ability to capture temporal dynamics. Further work will extend GazeVLM to videos by incorporating visual prompts to focus on regions of interest across frames. In addition, our goal is to improve the computational efficiency of GazeVLM for real-time applications. We plan to explore optimization mechanisms to enhance its practicality for real-world use.

References

- [1] Adria Recasens*, Aditya Khosla*, Carl Vondrick, and Antonio Torralba. Where are they looking? In *Advances in Neural Information Processing Systems (NIPS)*, 2015. * indicates equal contribution.
- [2] Francesco Tonini, Nicola Dall’Asen, Cigdem Beyan, and Elisa Ricci. Object-aware gaze target detection, 2023.
- [3] Samy Tafasca, Anshul Gupta, and Jean-Marc Odobez. Sharingan: A transformer architecture for multi-person gaze following. In *Proceedings of the IEEE/CVF Conference on Computer Vision and Pattern Recognition (CVPR)*, pages 2008–2017, 2024.
- [4] Anshul Gupta, Samy Tafasca, Arya Farkhondeh, Pierre Vuillecard, and Jean-Marc Odobez. Mtgs: A novel framework for multi-person temporal gaze following and social gaze prediction. In *Advances in Neural Information Processing Systems (NeurIPS)*, 2024.
- [5] Shreya Ghosh, Abhinav Dhall, Munawar Hayat, Jarrod Knibbe, and Qiang Ji. Automatic gaze analysis: A survey of deep learning based approaches. *IEEE Transactions on Pattern Analysis and Machine Intelligence*, 46(1):61–84, 2023.
- [6] Fiona Ryan, Ajay Bati, Sangmin Lee, Daniel Bolya, Judy Hoffman, and James M. Rehg. Gaze-Ile: Gaze target estimation via large-scale learned encoders, 2024.

- [7] Kun Yan, Zeyu Wang, Lei Ji, Yuntao Wang, Nan Duan, and Shuai Ma. Voila-a: Aligning vision-language models with user’s gaze attention. *Advances in Neural Information Processing Systems*, 37:1890–1918, 2024.
- [8] Anshul Gupta, Pierre Vuillecard, Arya Farkhondeh, and Jean-Marc Odobez. Exploring the zero-shot capabilities of vision-language models for improving gaze following. In *Proceedings of the IEEE/CVF Conference on Computer Vision and Pattern Recognition*, pages 615–624, 2024.
- [9] Peng Wang, Shuai Bai, Sinan Tan, Shijie Wang, Zhihao Fan, Jinze Bai, Keqin Chen, Xuejing Liu, Jialin Wang, Wenbin Ge, Yang Fan, Kai Dang, Mengfei Du, Xuancheng Ren, Rui Men, Dayiheng Liu, Chang Zhou, Jingren Zhou, and Junyang Lin. Qwen2-vl: Enhancing vision-language model’s perception of the world at any resolution, 2024.
- [10] Eunji Chong, Yongxin Wang, Nataniel Ruiz, and James M. Rehg. Detecting attended visual targets in video, 2020.
- [11] Binglu Wang, Chenxi Guo, Yang Jin, Haisheng Xia, and Nian Liu. Transgop: Transformer-based gaze object prediction, 2024.
- [12] Binglu Wang, Tao Hu, Baoshan Li, Xiaojuan Chen, and Zhijie Zhang. Gatecor: A unified framework for gaze object prediction. In *2022 IEEE/CVF Conference on Computer Vision and Pattern Recognition (CVPR)*, pages 19566–19575, 2022.
- [13] Samy Tafasca, Anshul Gupta, and Jean-Marc Odobez. Sharingan: A transformer architecture for multi-person gaze following. In *2024 IEEE/CVF Conference on Computer Vision and Pattern Recognition (CVPR)*, pages 2008–2017, 2024.
- [14] Nora Horanyi, Linfang Zheng, Eunji Chong, Aleš Leonardis, and Hyung Jin Chang. Where are they looking in the 3d space? In *2023 IEEE/CVF Conference on Computer Vision and Pattern Recognition Workshops (CVPRW)*, pages 2678–2687, 2023.
- [15] Shiwei Jin, Ji Dai, and Truong Nguyen. Kappa angle regression with ocular counter-rolling awareness for gaze estimation. In *2023 IEEE/CVF Conference on Computer Vision and Pattern Recognition Workshops (CVPRW)*, pages 2659–2668, 2023.
- [16] Ruicong Liu and Feng Lu. Uvagaze: Unsupervised 1-to-2 views adaptation for gaze estimation, 2023.
- [17] Swati Jindal, Mohit Yadav, and Roberto Manduchi. Spatio-temporal attention and gaussian processes for personalized video gaze estimation, 2024.
- [18] Hengfei Wang, Jun O Oh, Hyung Jin Chang, Jin Hee Na, Minwoo Tae, Zhongqun Zhang, and Sang-II Choi. Gazecaps: Gaze estimation with self-attention-routed capsules. In *2023 IEEE/CVF Conference on Computer Vision and Pattern Recognition Workshops (CVPRW)*, pages 2669–2677, 2023.
- [19] Liang Wu and Bertram E. Shi. Merging multiple datasets for improved appearance-based gaze estimation. In Apostolos Antonacopoulos, Subhasis Chaudhuri, Rama Chellappa, Cheng-Lin Liu, Saumik Bhattacharya, and Umapada Pal, editors, *Pattern Recognition*, pages 77–90, Cham, 2025. Springer Nature Switzerland.
- [20] Haldun Balim, Seonwook Park, Xi Wang, Xucong Zhang, and Otmar Hilliges. Efe: End-to-end frame-to-gaze estimation, 2023.
- [21] Danyang Tu, Xiongkuo Min, Huiyu Duan, Guodong Guo, Guangtao Zhai, and Wei Shen. End-to-end human-gaze-target detection with transformers. In *2022 IEEE/CVF Conference on Computer Vision and Pattern Recognition (CVPR)*, pages 2192–2200. IEEE, 2022.
- [22] Qiaomu Miao, Minh Hoai, and Dimitris Samaras. Patch-level gaze distribution prediction for gaze following. In *2023 IEEE/CVF Winter Conference on Applications of Computer Vision (WACV)*, pages 880–889, 2023.
- [23] Sounak Mondal, Zhibo Yang, Seoyoung Ahn, Dimitris Samaras, Gregory Zelinsky, and Minh Hoai. Gazeformer: Scalable, effective and fast prediction of goal-directed human attention, 2023.
- [24] Samy Tafasca, Anshul Gupta, and Jean-Marc Odobez. Childplay: A new benchmark for understanding children’s gaze behaviour. In *2023 IEEE/CVF International Conference on Computer Vision (ICCV)*, pages 20878–20889, 2023.
- [25] Anshul Gupta, Samy Tafasca, and Jean-Marc Odobez. A modular multimodal architecture for gaze target prediction: Application to privacy-sensitive settings. In *2022 IEEE/CVF Conference on Computer Vision and Pattern Recognition Workshops (CVPRW)*, pages 5037–5046, 2022.
- [26] Yuqi Hou, Zhongqun Zhang, Nora Horanyi, Jaewon Moon, Yihua Cheng, and Hyung Jin Chang. Multi-modal gaze following in conversational scenarios, 2023.

- [27] Ekta Sood, Fabian Kögel, Philipp Müller, Dominike Thomas, Mihai Băce, and Andreas Bulling. Multimodal integration of human-like attention in visual question answering. In *2023 IEEE/CVF Conference on Computer Vision and Pattern Recognition Workshops (CVPRW)*, pages 2648–2658, 2023.
- [28] Mathew Athul, Khan Arshad, Khalid Thariq, AL-Tam Farooq, and Souissi Riad. Leveraging multi-modal saliency and fusion for gaze target detection. In *NeuRIPS 2023 Workshop on Gaze Meets ML*, 2023.
- [29] Jianhang Chen, Xu Zhang, Yue Wu, Shalini Ghosh, Pradeep Natarajan, Shih-Fu Chang, and Jan Allebach. One-stage object referring with gaze estimation. In *2022 IEEE/CVF Conference on Computer Vision and Pattern Recognition Workshops (CVPRW)*, pages 5017–5026, 2022.
- [30] Yichen Shi, Feifei Zhang, Wenming Yang, Guijin Wang, and Nan Su. Agent-guided gaze estimation network by two-eye asymmetry exploration. In *2024 IEEE International Conference on Image Processing (ICIP)*, pages 2320–2326, 2024.
- [31] Mingfang Zhang, Yunfei Liu, and Feng LU. GazeOnce: Real-Time Multi-Person Gaze Estimation . In *2022 IEEE/CVF Conference on Computer Vision and Pattern Recognition (CVPR)*, pages 4187–4196, Los Alamitos, CA, USA, June 2022. IEEE Computer Society.
- [32] Yuehao Song, Xinggang Wang, Jingfeng Yao, Wenyu Liu, Jinglin Zhang, and Xiangmin Xu. Vitgaze: Gaze following with interaction features in vision transformers, 2024.
- [33] Jun Bao, Buyu Liu, and Jun Yu. Escnet: Gaze target detection with the understanding of 3d scenes. In *2022 IEEE/CVF Conference on Computer Vision and Pattern Recognition (CVPR)*, pages 14106–14115, 2022.
- [34] Junnan Li, Dongxu Li, Silvio Savarese, and Steven Hoi. Blip-2: Bootstrapping language-image pre-training with frozen image encoders and large language models, 2023.
- [35] Yizhou Wang, Yixuan Wu, Shixiang Tang, Weizhen He, Xun Guo, Feng Zhu, Lei Bai, Rui Zhao, Jian Wu, Tong He, and Wanli Ouyang. Hulk: A universal knowledge translator for human-centric tasks, 2024.
- [36] Yang Jin, Lei Zhang, Shi Yan, Bin Fan, and Binglu Wang. Boosting gaze object prediction via pixel-level supervision from vision foundation model, 2024.
- [37] OpenAI <https://github.com/openai/openai-python/blob/release/v0.28.0/chatml.md>.
- [38] Xingyi Zhou, Rohit Girdhar, Armand Joulin, Philipp Krähenbühl, and Ishan Misra. Detecting twenty-thousand classes using image-level supervision, 2022.
- [39] Agrim Gupta, Piotr Dollar, and Ross Girshick. LVIS: A dataset for large vocabulary instance segmentation. In *Proceedings of the IEEE Conference on Computer Vision and Pattern Recognition*, 2019.
- [40] Jinze Bai, Shuai Bai, Shusheng Yang, Shijie Wang, Sinan Tan, Peng Wang, Junyang Lin, Chang Zhou, and Jingren Zhou. Qwen-vl: A versatile vision-language model for understanding, localization, text reading, and beyond, 2023.
- [41] René Ranftl, Katrin Lasinger, David Hafner, Konrad Schindler, and Vladlen Koltun. Towards robust monocular depth estimation: Mixing datasets for zero-shot cross-dataset transfer. *IEEE Transactions on Pattern Analysis and Machine Intelligence*, 44(3), 2022.
- [42] Saurabh Gupta, Ross Girshick, Pablo Arbeláez, and Jitendra Malik. Learning rich features from rgb-d images for object detection and segmentation, 2014.
- [43] Eunji Chong, Nataniel Ruiz, Yongxin Wang, Yun Zhang, Agata Rozga, and James M. Rehg. Connecting gaze, scene, and attention: Generalized attention estimation via joint modeling of gaze and scene saliency. In *Computer Vision – ECCV 2018: 15th European Conference, Munich, Germany, September 8–14, 2018, Proceedings, Part V*, page 397–412, Berlin, Heidelberg, 2018. Springer-Verlag.
- [44] Dongze Lian, Zehao Yu, and Shenghua Gao. Believe it or not, we know what you are looking at! In C. V. Jawahar, Hongdong Li, Greg Mori, and Konrad Schindler, editors, *Computer Vision – ACCV 2018*, pages 35–50, Cham, 2019. Springer International Publishing.
- [45] Yi Fang, Jiapeng Tang, Wang Shen, Wei Shen, Xiao Gu, Li Song, and Guangtao Zhai. Dual attention guided gaze target detection in the wild. In *2021 IEEE/CVF Conference on Computer Vision and Pattern Recognition (CVPR)*, pages 11385–11394, 2021.
- [46] Francesco Tonini, Cigdem Beyan, and Elisa Ricci. Multimodal across domains gaze target detection. In *Proceedings of the 2022 International Conference on Multimodal Interaction, ICMI ’22*, page 420–431. ACM, November 2022.